Synthesis of Magnetic Multiwalled Carbon Nano Tubes and Investigation of isotherm and kinetic models for cleanup of Carbaryl pesticide

Ramin Khaghani[1], Ali Esrafili[2], Dariush Zeynalzadeh[3, 4*], Farshad Bahrami Asl[5]

1-School of medicine, AJA University of Medical Sciences, Tehran, Iran, Email: khagha_r@yahoo.com Tel: +98 21 85952211

2- Department of Environmental Health Engineering, Faculty of Public Health, Iran University of Medical Sciences, Tehran, Iran, Email: a_srafili@yahoo.com Tel: +982186704627; Fax: +982188622707

3- Researcher, School of medicine, AJA University of Medical Sciences, Tehran, Iran, Email: d.zeynalzadeh@yahoo.com Tel: +989147204630

4-Department of Environmental Health Engineering, Faculty of Public Health, Tehran University of Medical Sciences, Tehran, Iran; Fax: +984143343322

5-Department of Environmental Health Engineering, School of Public Health, Urmia University of Medical Sciences, Urmia, Iran, Email: farshadfba@gmail.com Tel: +984432784378; Fax: +9802188622707

GRAPHICAL ABSTRACT

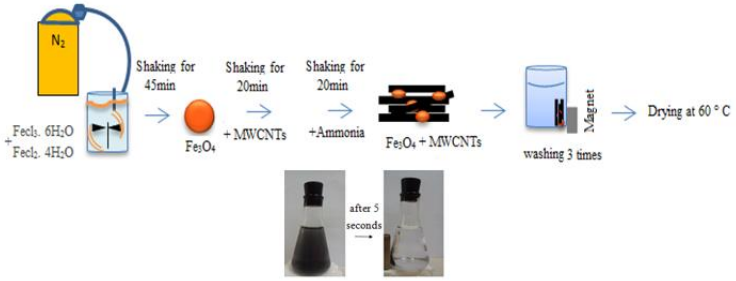

Abstract: Water is the main factor of movement and transport of pesticides and contamination of water by these pollutants is one of the most important challenges due to their widespread use and increased concentrations. Moreover, these compounds are on the U.S.EPA Priority Pollutant list because of the potential of accumulation and the property of damaging effects. In this study, multiwalled carbon nanotube-based magnetic nanoparticles were synthesized and used as an affective adsorbent for carbaryl pesticide. The properties of the synthesized Fe_3O_4@MWCNTs were characterized by TEM images and XRD analysis. The obtained data were studied by isotherm and kinetic models. Carbaryl adsorbed onto the synthesized adsorbent was compatible with the Langmuir isotherm (R^2 =0.993). The maximum adsorption capacity (q_{max}) of the pesticide onto the Fe_3O_4-MWCNTs was obtained at 68.2 mg/g. The kinetic studies of the reactions showed that the adsorption process followed the pseudo-second order model with $R^2 \geq 0.99$ for all initial carbaryl concentrations. The adsorbent was extracted by magnet reused several times (six rounds) with a reasonable efficiency. The Fe_3O_4-MWCNTs have great potential for adsorption of carbaryl from water and wastewater due to high efficiency, easy separation and reusability.

Keywords: Adsorption, Carbon Nanotube, Carbaryl, Kinetic, Isotherm

1. Introduction

Carbamates are one of the major classes of the pesticides, which are widely used in agriculture against insects, fungi and weeds(Wu et al. 2010; Liu et al. 2009). These compounds are potentially hazardous to

the environment and human health. Carbaryl (1-naphthyl-N-methyl carbamate) (scheme.1), which is a broad-spectrum insecticide, is used to control more than 100 species of insects in fruits, forests, lawns, domestic vegetables and other crops (Melchert and Rocha 2010; Zhu et al. 2009). This compound, because of their ability to accumulate and their long-term effects on living organisms, is on the priory list released by the USEPA[1] (Chin-Chen et al. 2012; Alavanja, Hoppin, and Kamel 2004; Liu, Zheng, and Li 2013). The potential risks of human health owing to the contact with pesticides are noticeably seen through the detection of pesticide compounds residues in water, foodstuffs and even in breast milk (El Ouardi et al. 2013). Carbaryl can cause adverse effects on humans with inhalation, skin contact, or ingestion (Chin-Chen et al. 2012). Exposure to this substance, in addition to its teratogenic characteristics, inhibits the cholinesterase enzyme, impairing the functions of the central nervous system and can cause nausea, vomit, broncho-constriction, blurred vision, convulsions, coma and respiratory failure (Chowdhury et al. 2012; Melchert and Rocha 2010; Liu, Zheng, and Li 2013).

In soil, carbaryl is bounded by organic materials and can be transported (Ghauch et al. 2001). Removal of these organic pollutants during water treatment has been tested through nanofiltration (Boussahel et al. 2000), ozonation (Kusvuran et al. 2012) and some of adsorbents such as activated carbon (El Ouardi et al. 2013; Zhang et al. 2012; Meyers, Ahlrichs, and White 2013; Chen et al. 2009). However, these techniques have some disadvantages like rapidly saturated for some adsorbents and generated byproducts. Carbon nanotubes (CNTs), due to their high surface area, have long been employed as adsorbents for trapping or separation of some contaminants from aquatic environments. But their large-scale application has somewhat been limited owing to the problems in separating materials (products and residual sorbents) from solution (Jiang et al. 2009; Wu et al. 2011). CNTs display excellent mechanical, electrical and magnetic properties (Sahoo et al. 2010).

Recently, the magnetic separation method has been applied due to its low cost, economic aspects, biodegradability, non-toxicity, simplicity and being quick in separation (Kakavandi et al. 2013; Prucek et al. 2011; Mi et al. 2011; Dong et al. 2012). In this study, we synthesized and used super paramagnetic Fe_3O_4 nanoparticles in order to produce magnetic separation characteristic for MWCNTs[2].

Moreover, the mechanisms of adsorption of solutions of carbaryl, as an effluent model, and magnetic MWCNTs, as the adsorbents, were chosen to be studied. Therefore, after Carbaryl sorption onto the Fe_3O_4-MWCNTs nanoparticles, the adsorbents could be readily separated from water solution with an external magnetic field. The basic objectives of the present work were as follows: (1) synthesizing Fe_3O_4-MWCNTs and presenting its properties, (2) investigating the adsorption kinetics and analyzing the experimental data with the pseudo-first-order and pseudo-second-order equations, (3) investigating the adsorption isotherms and analyzing experimental data with the Langmuir, Freundlich and BET models and (4) implementing reuse of Fe_3O_4- MWCNTs after adsorption.

2. Experimental

2.1 Adsorbate

Technical grade Carbaryl ($C_{12}H_{11}NO_2$) of 99.9% purity supplied by Sigma-Aldrich was used as an adsorbate. The structure of the insecticide has been shown in scheme 1. Distilled water was used to prepare all solutions.

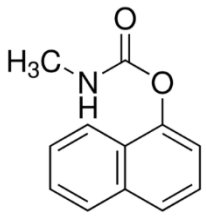

Scheme.1. Chemical structure of Carbaryl

[1] United States Environmental Protection Agency

[2] Multi Walled Carbon Nano Tubes

2.2 Material

Multiwalled carbon nanotubes were prepared from nano US Company, ferric chloride hexahydrate ($Fecl_3.6H_2O$), ferrous chloride tetrahydrate ($Fecl_2.4H_2O$) and ammonia were purchased from Merck (Germany).

2.3 Apparatus

The HPLC[3], assembled from modular components (CECIL, CE4100, England), consisted of an in-line degasser, a 600E pump and a UV-visible detector (CE4200, CECIL, England). The injection loop volume was 30 µL. A C_{18ec} column (250 mm×4.6 mm I.D., 5.0 µm) MACHERY-NAGEL (German Quality) was used for separations. The mobile phase was a combination of methanol–water (70:30, v/v) at the flow rate of 1mL/min. UV detector wavelengths were selected at 220 nm for carbaryl. The identification of carbaryl was made by retention times and ultraviolet absorption spectra detection. The peak area of the analyte was used for quantification.
The morphology of MWCNTs and Fe_3O_4-MWCNTs was characterized by transmission electron microscope (TEM) images (obtained with EM 208-Philips operated at an acceleration voltage of 100 kV). X-ray diffraction (XRD) measurement was performed using a Bruker D8Advance (CuK, radiation with 1.5416A˚ wavelengths) diffractometer. In order to do magnetic separation of adsorbent from aqueous solution, we used a magnetic field with the intensity of 1.3 T; and, a pH meter (HACH-HQ-USA) was used to control solution pH (±0.01).

2.4 Synthesis of Fe_3O_4-CNTs

Magnetic carbon Nanotubes were synthesized by a co-precipitation method. $FeCl_3.6H_2O$ (8.48 gr) and $Fecl_2 4H_2O$ (2.25 gr) were dissolved in 400 ml water and mixed by mechanical stirring; then, the samples were heated at 75 °C within 45min under nitrogen gas. Next, after homogenization in ultrasonic, 10 gr MWCNTs, were added to the solution and kept for 20 min. Afterwards, 20 ml ammonia was added to the solution. After 20 min, the Fe_3O_4-MWCNTs were separated with an external magnet and washed three times with distilled water. Finally, the nanoparticles were dried in a vacuum oven at 60 °C within 6 hours. The preparation procedure of the magnetic carbon nanotubes has been illustrated in Fig 1.

2.5 Adsorption kinetic and isotherm study

The parameters investigated in the current study were pH, adsorbent dose (Fe_3O_4-MWCNTs), initial carbaryl concentration and contact time. For kinetic studies, a series of 100-mL Erlenmeyer flasks were filled with 50 mL the pesticide solution at the concentration of 10 mg/L. The pH of the solution was kept at 6 by adding 0.1 M NaOH or 0.1M HNO_3. An equal amount of the adsorbent (0.2 g/L) was added separately to each flask. The agitation speed was kept constant at 150 rpm. At predetermined intervals of time (5, 10, 15, 20, 25, 30, 60 and 120 min), Fe_3O_4-MWCNTs were separated from the solution by an external magnet field.

Adsorption isotherm experiments were conducted by adding 50 mL of the solution containing 10 mg/L pesticide to different concentrations of the adsorbent (0.1, 0.15, 0.2, 0.25, 0.3 and 0.5 g/L). The mixtures were kept until 30 min at the pH value of 6.

The standard coefficient of determination (R^2) was employed to compare the amount of fitting between prediction models and measured data.

3. Result and discussion

3.1 Characterization of magnetic carbon nanotubes

[3] High-performance liquid chromatography

X-ray diffraction (XRD) measurements were employed to investigate the phase and structure of the MWCNTs and synthesized Fe_3O_4-MWCNTs. Diffraction peaks assigned to MWCNTs at $2\theta = 26.5^{\circ}$(Fig. 2a) can be clearly seen in the XRD curves of pure MWCNT (Wang et al. 2008), and the Fe_3O_4-MWCNT composite indicating the MWCNT structure was not destroyed after the successive deposition of Fe_3O_4. From Fig. 2b, except for the diffraction peak at $2\theta=26.5^{\circ}$resulting from MWCNTs, all the new significant diffraction peaks of the Fe_3O_4-MWCNT, which are matched well with the data for Fe_3O_4: 30.2°, 35.6°, 43.3°, 53.7°, 57.3°, and 62.8°, can be assigned to (2 2 0), (3 1 1), (4 0 0), (4 2 2), (5 1 1), and (4 4 0) of the crystal indices for Fe_3O_4, respectively.

TEM images of MWCNTs and Fe_3O_4-MWCNTs have been shown in Fig 3. The outer diameters of those tubes are in the approximate range of 10–30 nm. As shown in Fig 3b, the iron oxide nanoparticles were coated on the surface of MWCNTs to form Fe_3O_4-MWCNTs. The Fe_3O_4 nanoparticles were properly distributed on the surface of the carbon tubes.

3.2 Adsorption isotherms modeling

Three isotherms: Langmuir, Freundlich and Brunauer–Emmett–Teller (BET) were tested for their ability for description of the experimental results. The Langmuir isotherm is founded on the assumption that the adsorption process takes place on homogenous adsorbent surfaces (Kakavandi et al. 2013). This model assumes that maximum adsorption corresponds to a saturated monolayer of solute molecules on the surface of the adsorbent, with no lateral interaction among the sorbed molecules. The linear equation of the Langmuir model is shown as Eq.1:

$$\frac{1}{q_e} = \frac{1}{q_{max}} + \frac{1}{b\,C_e q_{max}} \qquad (1)$$

Where q_e (mg/g) is the amount of sorbed molecules per unit mass of the adsorbent, C_e (mg/L) is the adsorbate concentration at equilibrium, q_{max} (mg/g) is the maximum amount of the adsorbate per unit mass of adsorbent when complete monolayer bound at high C_e and b (L/mg) is the Langmuir constant. Fig 4 shows that the adsorption of carbaryl onto Fe_3O_4-MWCNTs was best fitted to the Langmuir model. The Langmuir constants (b) and q_{max} were obtained from the intercept and slope of the plot. Characteristics of the Langmuir model can be descripted with the R_L factor as shown in Eq.2 (Hameed, Salman, and Ahmad 2009):

$$R_L = \frac{1}{1+bc_0} \qquad (2)$$

Where C_0 is the maximum initial dose of the adsorbate (mg/L). The factor of R_L represents the condition of the isotherm to be irreversible (RL=0), favorable (0< RL >1), linear adsorption (RL=1) and unfavorable (RL >1). The value of R_L in the present investigation was found to be 0.33 indicating that the adsorption of carbaryl onto Fe_3O_4-MWCNTs is favorable.

The BET model (Classics Brunauer, Emmett, and Teller 1938) is a development of the Langmuir model for multilayer adsorption. The BET isotherm is a theoretical equation and are commonly employed in the gas–solid equilibrium processes. It assumes that each adsorbate in the first adsorbed layer serves as an adsorption site for the second layer and so forth (Ofomaja, Unuabonah, and Oladoja 2010). In this study, this model was used to calculate Carbaryl sorption based on Eq. (3):

$$\frac{c_e}{(c_s-c_e)q} = \frac{1}{K_{BET}q_m} + \left(\frac{K_{BET}-1}{K_{BET}q_m}\right)\left(\frac{c_e}{c_s}\right) \qquad (3)$$

where K_{BET}, c_s, q_m and q are the constant expressive of energy of interaction with the surface, adsorbate monolayer saturation concentration (mg/L), theoretical isotherm saturation capacity (mg/g) and equilibrium adsorption capacity (mg/g), respectively. A plot of $C_e/(C_s–C_e)q$ against (C_e/C_s) should give a straight line. The values of K_{BET} and q_m can be calculated from the slope and intercept (fig.5).

The third model is the Freundlich approach; according to this model, the uptake of sorbate fall out on a heterogeneous surface by multilayer sorption (Freundlich and Hatfield 1926). The linear form of this model is presented by Eq. 4.

$$\text{Ln } q_e = \ln K_f + \frac{1}{n} \ln C_e \qquad (4)$$

Where K_F (L/g) is the constant showing the relative adsorption capacity of the adsorbent and 1/n is the intensity of the adsorption. K_F and n are calculated from the intercept and slope of the plot.

As can be seen from Table 1, the Freundlich model does not fit well the experimental data ($R^2 < 0.95$). Thus, carbaryl adsorption onto the magnetic carbon nanotubes cannot be expressed by the Freundlich isotherm. For the Freundlich isotherm model, the value of n was greater than 1 illustrating that the adsorption process followed a normal Langmuir isotherm. This shows homogeneous magnetic carbon nanotube surface in which the carbaryl molecule and carbon nanotubes had equal adsorption activation energy (Salman and Hameed 2010).

The correlation coefficient (R^2 values) was used to judge the applicability of the isotherm equation. As seen in Table 1, the Langmuir isotherm was best fitted to the experimental data while fitting the Freundlich isotherm represents a multilayer adsorption and the BET isotherm, which is an extension of the Langmuir isotherm, shows that multilayer sorption is not as good as the Langmuir model for carbaryl toxin adsorption.

The adsorption isotherm models fitted the data in the order of: Langmuir > Freundlich > BET isotherm.

3.3. Comparison of carbaryl adsorption capacity among different adsorbents

Table 2 compares the adsorption capacity of different types of adsorbents reported in the literature for adsorption of some pesticides. It is apparent that recycled Fe_3O_4-MWCNTs are very useful adsorbent for carbaryl removal from aqueous solutions. The value of q_{max} in this study is larger than that in most of previous works. This suggests that carbaryl could easily be adsorbed by the magnetic nanotubes.

3.4. Adsorption kinetic modeling

This study examined the kinetics of carbaryl removal from solutions by magnetic carbon nanotubes through the pseudo-first order and second order kinetic models as shown in Eqs. (6) and (7), respectively [28].

$$\text{Log } (q_e - q_t) = \log q_e - \frac{k_1}{2.303} t \qquad (6)$$

$$\frac{t}{q_t} = \frac{1}{k_2 q_e^2} + \frac{t}{q_e} \qquad (7)$$

Where q_t (mg/g) is the adsorption at time t (min), q_e (mg/g) is the adsorption capacity at adsorption equilibrium and k_1 (min^{-1}) and k_2 (g mg^{-1} min^{-1}) are the kinetic rate constants for the pseudo-first-order and the pseudo-second-order models, respectively. The Lagergren's first-order rate constant (k_1) and qe determined from the model have been presented in Table 3 with the corresponding correlation coefficients. The correlation coefficients (R^2) for the pseudo-second-order adsorption model were all higher than for the pseudo-first-order model. As can be seen from Table 3, there is no agreement between q_e experimental and q_e calculated values for the pseudo-first-order model.

The linear plots of t/q_t versus t have been shown in Fig 7 for the pseudo-second-order kinetic, yielded R^2 values >0.99 for all carbaryl concentrations and this showed a good agreement between the experimental and the calculated q_e values (table 3). Similar findings were claimed for carbofuran adsorption from aqueous environment through activated carbon (Salman and Hameed 2010).

3.5. Effect of solution pH

The effect of pH on carbaryl adsorption was investigated using 10 mg/L of initial concentration, and pH between 2 and10 at 22 °C. The equilibrium adsorption (q_e) was found to decline when pH increased (Fig

8). The q_e increased from 37.7 to 48.1 mg/g when pH value ranged between 2 and 10. Different physical/chemical processes like hydrolysis, complexation of ligands, redox reactions and precipitation are highly affected with pH (Mahapatra, Mishra, and Hota 2013). The pesticide adsorption onto Fe_3O_4-MWCNTs increased abruptly at pH ranging from 2 to 4; then, it increased slowly at pH from 4 to 10. At lower pH, the concentration of H^+ ion is high. Thus, it significantly influenced the protonation–deprotonation transition of MWCNT surface groups like –OH and –COOH, resulting in a competition for vacant adsorbent sites between H^+ ion and adsorbate molecules; for this reason, at low pH, the removal efficiency is low. Yang et al. claimed a similar pH effect on adsorption phenolic compounds adsorption trend by means of MWCNTs adsorbent (Yang et al. 2008).

3.6. Effect of contact time and initial concentration on carbaryl adsorption

The effects of time and initial concentration of carbaryl on the uptake using magnetic carbon nano tubes have been presented in Fig 9. The equilibrium was achieved at 30 min for carbaryl adsorption onto Fe_3O_4-MWCNTs. The time of equilibration adsorption was unaffected with initial concentration, but the amount adsorbed increased by increasing initial concentration of the pesticide. An increase in adsorption was observed from 24, 35.2 and 90 mg/g for initial concentrations of 5, 10 and 20 mg/L, respectively. This illustrates that initial concentration is very important in carbaryl adsorption on Fe_3O_4-MWCNTs. This is due to the fact that, at higher initial concentrations, carbaryl has to diffuse to the inner sites of the carbon nano tubes. Gubta et al.(Gupta et al. 2011) investigated the effect of the parameter initial concentration on adsorption of pesticides by activated carbon and they reported similar observations.

3.7. Reusability of Fe_3O_4-MWCNTs

The main objective of the reuse process is to restore the adsorption capacity of an exhausted adsorbent. The repeated availability of Fe_3O_4-MWCNTs for carbaryl adsorption from aqueous solution through many cycles of adsorption/desorption is quite crucial for the application of magnetic MWCNTs in the removal of pesticides from solution in real work. In this study, the reuse of Fe_3O_4- MWCNTs, each time after washing with distilled water, in the removal of carbaryl from aqueous solution was examined. Adsorption cycles repeated five times by using the same adsorbent for the new samples of the pesticide. Fig 10 presents adsorption percentages after reuse.

It is observed that the adsorption percentage of carbaryl declined from 94 to 77% with increasing the times of the reuse. The removal efficiency of the pesticide onto Fe_3O_4-MWCNTs was well after reuse for four times, which illustrates that the MWCNTs have a very good reusability.

4. Conclusion

Multi-walled carbon nano tube-based magnetic nanocomposite was synthesized and it was used as an effective adsorbent for carbaryl pesticide for the first time. The XRD analysis and TEM images of the CNTs and Fe_3O_4-MWCNTs confirm the formation of the synthesized nanocomposite. The equilibrium data were fitted to the Langmuir, Freundlich and BET isotherm models. The suitability of the kinetic models for the adsorption of the pesticide was also discussed. It was found that the adsorption kinetics obeyed the pseudo-second-order adsorption kinetic model. After sorption, the adsorbent can be extracted and be efficiently reused for many cycles.

References

Al-Qodah Z., Shawaqfeh A.T. and Lafi W.K. (2007), Adsorption of pesticides from aqueous solutions using oil shale ash, *Desalination*, 208, 294-305.

Alavanja M.C.R., Jane A.H. and Freya K. (2004), Health Effects of Chronic Pesticide Exposure: Cancer and Neurotoxicity* 3, *Annu. Rev. Public Health*, 25, 155-97.

Boussahel R., Bouland S., Moussaoui K.M. and Montiel A. (2000), Removal of pesticide residues in water using the nanofiltration process, *Desalination*, 132, 205-09.

Chen H., Xiaomin H., Xingmin R., Wenli C., Peng C., Wei L., Shengqing L.i. and Qiaoyun H. (2009), Adsorption and biodegradation of carbaryl on montmorillonite, kaolinite and goethite, *Applied clay science*, 46, 102-08.

Chen C., Liang M., Alegre M.R., Durgbanshi A., Bose D., Mourya K.S., Romero J.E. and Carda-Broch S. (2012), Micellar Liquid Chromatographic Determination of Carbaryl and 1-Naphthol in Water, Soil, and Vegetables, *International journal of analytical chemistry*, 2012.

Chowdhury A. Z., Jahan S. A., Islam M.N., Moniruzzaman M., Alam M.K., Zaman M.A., Karim N. and Gan S.H. (2012), Occurrence of organophosphorus and carbamate pesticide residues in surface water samples from the Rangpur district of Bangladesh, *Bulletin of environmental contamination and toxicology*, 89, 202-07.

Brunauer C., Emmett S.PH. and Teller E. (1938), Adsorption of gases in multimolecular layers, *Journal of the American Chemical Society*, 60, 309-19.

Dong J., Tao L., Xiaomeng M., Jianying Z., Kun S., Shiyun A. and Shenglong C. (2012), Amperometric biosensor based on immobilization of acetylcholinesterase via specific binding on biocompatible boronic acid-functionalized Fe@ Au magnetic nanoparticles, *Journal of Solid State Electrochemistry*, 16, 3783-90.

Bakouri El., Usero H.J., Morillo J., Rojas R. and Ouassini A. (2009), Drin pesticides removal from aqueous solutions using acid-treated date stones, *Bioresource technology*, 100, 2676-84.

Mahmoud El. O., Alahiane S., Qourzal S., Abaamrane A., Assabbane A. and Douch J. (2013), Removal of Carbaryl Pesticide from Aqueous Solution by Adsorption on Local Clay in Agadir, *American Journal of Analytical Chemistry*, 4, 72-79.

Freundlich H. and Hatfield H.S. (1926), Colloid and capillary chemistry.

Ghauch A., Gallet C., Charef A., Rima J. and Bouyer M. (2001), Reductive degradation of carbaryl in water by zero-valent iron, *Chemosphere*, 42, 419-24.

Gupta, V.K., Gupta B., Rastogi A., Agarwal Sh. and Nayak A. (2011), Pesticides removal from waste water by activated carbon prepared from waste rubber tire, *Water Research*, 45, 4047-55.

Hamadi N.K., Swaminathan S. and Chen X.D. (2004), Adsorption of paraquat dichloride from aqueous solution by activated carbon derived from used tires, *Journal of hazardous materials*, 112, 133-41.

Hameed B.H., Salman J.M. and Ahmad A.L. (2009), Adsorption isotherm and kinetic modeling of 2, 4-D pesticide on activated carbon derived from date stones, *Journal of hazardous materials*, 163, 121-26.

Jiang, C.J.C., Chen M.C.M., Xuan S.X.S., Jiang W.J.W., Gong X.G.X. and Zhang Z.Z.Z. (2009), Magnetic separable PSA@ Fe3O4/Ag composites-Fabrication and catalytic properties, *Canadian Journal of Chemistry*, 87, 502-06.

Kakavandi, B., Jonidi Jafari A., Rezaei Kalantary R., Nasseri S., Ameri A. and Esrafily A. (2013), Synthesis and properties of Fe3O4-activated carbon magnetic nanoparticles for removal of aniline from aqueous solution: equilibrium, kinetic and thermodynamic studies, *Iranian journal of environmental health science & engineering*, 10, 19-19.

Kusvuran E., Yildirim D., Mavruk F. and Ceyhan M. (2012), Removal of chloropyrifos ethyl, tetradifon and chlorothalonil pesticide residues from citrus by using ozone, *Journal of hazardous materials*.

Liu S., Zheng Z. and Li X. (2013), Advances in pesticide biosensors: current status, challenges, and future perspectives, *Analytical and bioanalytical chemistry*, 405, 63-90.

Liu Z. M, Xiao H. Z., Wei H. L., Chun W. and Zhi W. (2009), Novel method for the determination of five carbamate pesticides in water samples by dispersive liquid–liquid microextraction combined with high performance liquid chromatography, *Chinese Chemical Letters*, 20, 213-16.

Mahapatra A., Mishra B.G. and Hota G. (2013), Electrospun Fe2O3-Al2O3 nanocomposite fibers as efficient adsorbent for removal of heavy metal ions from aqueous solution, *Journal of hazardous materials*, 258, 116-23.

Mahmoud E.l., Said O.A., Samir Q., Abaamrane A., Assabbane A. and Douch J. (2013) Removal of carbaryl pesticide from aqueous solution by adsorption on local clay in Agadir, *American Journal of Analytical Chemistry*, 4, 72.

Mekhloufi M., Zehhaf A., Benyoucef A., Quijada C. and Morallon E. (2013), Removal of 8-quinolinecarboxylic acid pesticide from aqueous solution by adsorption on activated montmorillonites, *Environmental monitoring and assessment*, 185, 365-75.

Melchert W.R., and Rocha F.R.P. (2010), A greener and highly sensitive flow-based procedure for carbaryl determination exploiting long pathlength spectrophotometry and photochemical waste degradation, *Talanta*, 81, 327-33.

Meyers N.L., Ahlrichs J.L., and White J.L. (2013), Adsorption of Insecticides on Pond Sediments and Watershed Soils, In *Proceedings of the Indiana Academy of Science*, 432-38.

Mi, H., Xu Y., Shi W., Yoo H., Chae O.B. and Oh S.M. (2011), Flocculant–assisted synthesis of Fe2O3 carbon composites for superior lithium rechargeable batteries, *Materials Research Bulletin*.

Ofomaja A.E., Unuabonah E.I. and Oladoja N.A. (2010), Competitive modeling for the biosorptive removal of copper and lead ions from aqueous solution by Mansonia wood sawdust, *Bioresource Technology*, 101, 3844-52.

Prucek R., Tuček J., Kilianová M., Panáček A., Kvítek L., Filip J., Kolář M., Tománková K. and Zbořil R. (2011), The targeted antibacterial and antifungal properties of magnetic nanocomposite of iron oxide and silver nanoparticles, *Biomaterials*, 32, 4704-13.

Sahoo N.G., Sravendra R., Jae W. Ch., Lin L. and Siew H.Ch. (2010), Polymer nanocomposites based on functionalized carbon nanotubes', *Progress in polymer science*, 35, 837-67.

Salman J.M. and Hameed B.H. (2010), Removal of insecticide carbofuran from aqueous solutions by banana stalks activated carbon, *Journal of hazardous materials*, 176, 814-19.

Wang Sh., Huimin B., Pengyuan Y. and Gang Ch. (2008), Immobilization of trypsin in polyaniline-coated nano-Fe3O4 carbon nanotube composite for protein digestion, *Analytica chimica acta*, 612, 182-89.

Wu Q., Chang Q., Wu Ch., Rao H., Zeng X., Wang Ch. and Wang Z. (2010), Ultrasound-assisted surfactant-enhanced emulsification microextraction for the determination of carbamate pesticides in water samples by high performance liquid chromatography, *Journal of Chromatography A*, 1217, 1773-78.

Wu Q., Guangying Z., Cheng F., Chun W. and Zhi W. (2011), Preparation of a graphene-based magnetic nanocomposite for the extraction of carbamate pesticides from environmental water samples, *Journal of Chromatography A*, 1218, 7936-42.

Yang K., Wu W., Jing Q. and Zhu L. (2008), Aqueous adsorption of aniline, phenol, and their substitutes by multi-walled carbon nanotubes, *Environmental science & technology*, 42, 7931-36.

Zhang P., Sun H., Yu L. and Sun T. (2012), Adsorption and Catalytic Hydrolysis of Carbaryl and Atrazine on Pig Manure–Derived Biochars: Impact of Structural Properties of Biochars, *Journal of hazardous materials*.

Zhu Sh.H., Wu H.L., Xia A.L., Nie J.F., Bian Y.C., - Cai C.B. and Yu R.Q. (2009), Excitation-emission-kinetic fluorescence coupled with third-order calibration for quantifying carbaryl and investigating the hydrolysis in effluent water, *Talanta*, 77, 1640-46.

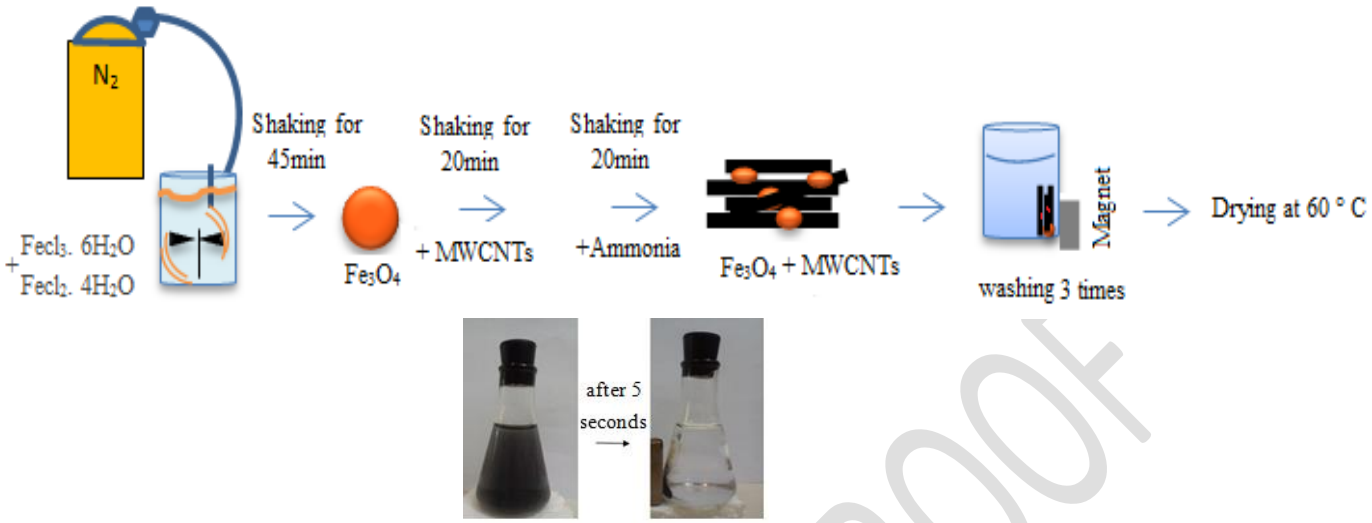

Fig. 1. Steps of synthesis of Fe_3O_4-MWCNTs magnetic Nano composites

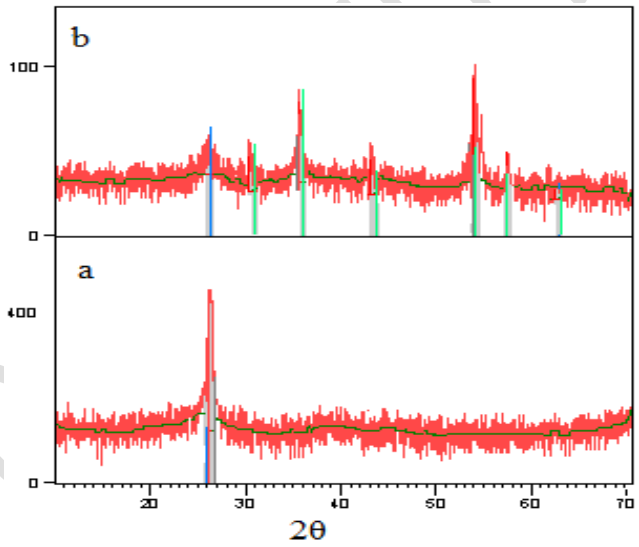

Fig. 2. X-ray diffraction pattern of (a) MWCNT and (b) Fe_3O_4–MWCNT

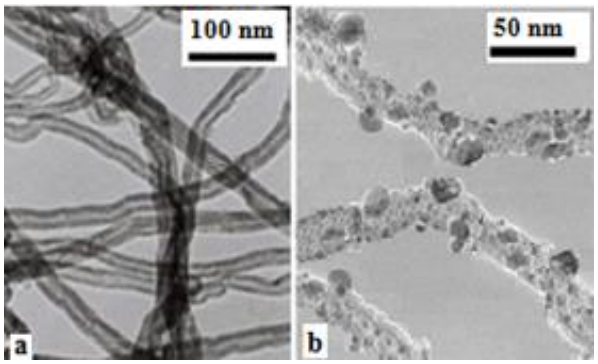

Fig. 3. TEM images of (a) MWCNTs and (b) Fe_3O_4-MWCNTs

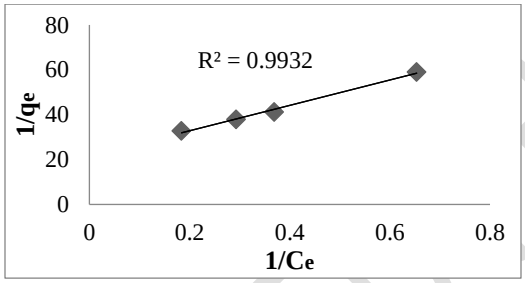

Fig. 4. Langmuir adsorption isotherm of Carbaryl on Fe_3O_4-CNTs

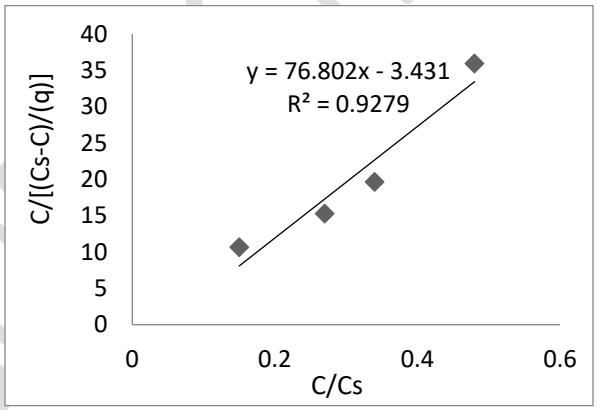

Fig. 5. BET adsorption isotherm of Carbaryl on Fe_3O_4-CNTs

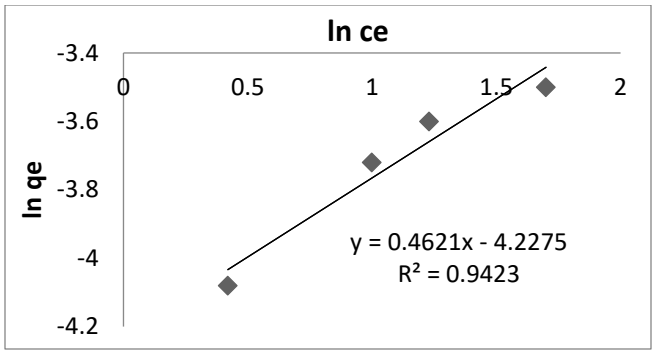

Fig. 6. Freundlich adsorption isotherm of Carbaryl on Fe_3O_4-MWCNTs

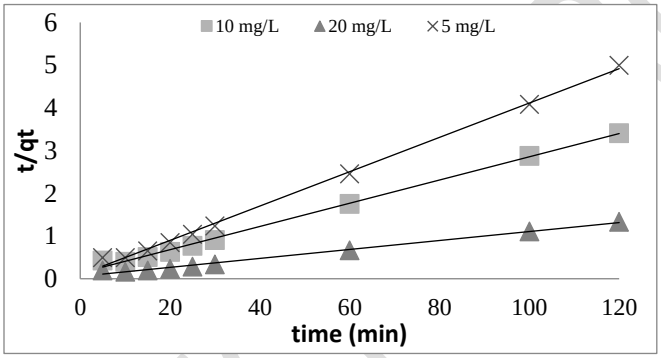

Fig. 7. Pseudo-second-order kinetics for adsorption of Carbaryl onto Fe_3O_4-MWCNTs

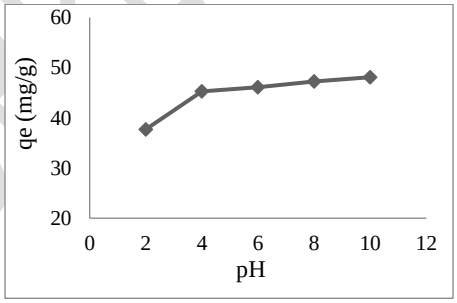

Fig. 8. Effect of solution pH on the uptake of Carbaryl

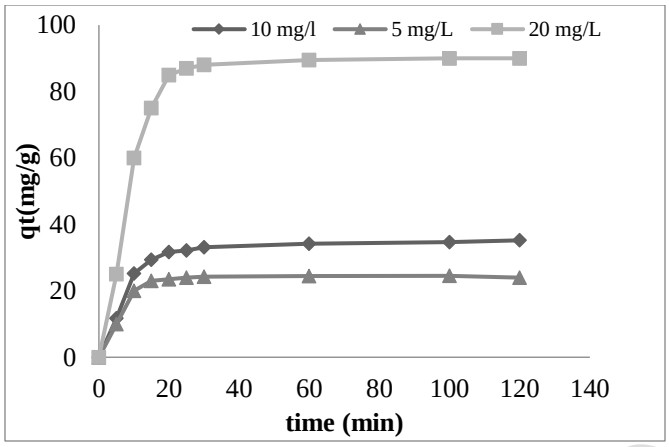

Fig. 9. Effect of initial concentration of Carbaryl adsorption onto Fe_3O_4- MWCNTs
Lines represents the model fitting of pseudo-second-order equation

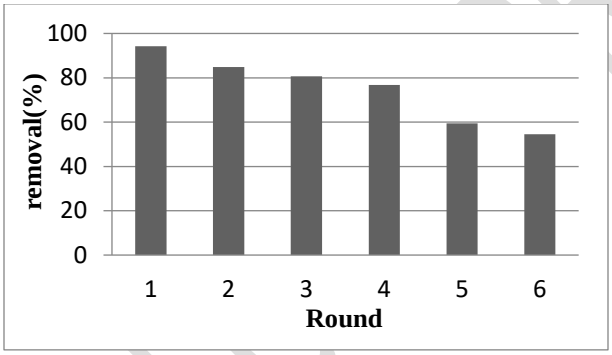

Fig. 10. Recycling use of Fe_3O_4-MWCNTs in the removal of Carbaryl from aqueous solution

Table1. Isotherm parameters for removal of Carbaryl by Fe_3O_4-CNTs

Isotherm	Parameters
Langmuir	
q_{max} (mg/g)	68.2
b (L/mg)	0.212
R^2	0.9932
Freundlich	
K_f	12.64
n	1.51
R^2	0.9423
BET	
K_{BET}	20.847
q_m	18.783
R^2	0.9279

Table 2.Comparison of adsorption capacity of different pesticides mentioned in this work and previous studies

Pesticide	Adsorbent	Qmax	R2	reference
carbaryl	Fe_3O_4-MWCNTs	68.2	0.993	The current study
carbaryl	Clay	10.75	0.97	(Mahmoud El et al. 2013)
Methyl parathion	Activated carbon	97.09	0.998	(Gupta et al. 2011)
Atrazine	Activated carbon	95.24	0.995	(Gupta et al. 2011)
Methoxychlor	Activated carbon	66.67	0.995	(Gupta et al. 2011)
Deltamethrin	oil shale ash	10.74	0.997	(Al-Qodah, Shawaqfeh and Lafi 2007)
Paraquat dichloride	Pyrolysis and activation of used tires	27.8	0.991	(Hamadi, Swaminathan and Chen 2004)
8-quinolinecarboxylic acid	Sodium montmorillonite	65.4	0.98	(Mekhloufi et al. 2013)
8-quinolinecarboxylic acid	Organic-acidic montmorillonite	75.9	0.99	(Mekhloufi et al. 2013)
Carbaforan	banana stalks activated carbon	161.3	0.989	(Salman and Hameed 2010)
Aldrin	acid-treated date stones	6.37	0.913	(El Bakouri et al. 2009)
Dieldrin	acid-treated date stones	6.97	0.901	(El Bakouri et al. 2009)
Endrin	acid-treated date stones	5.98	0.924	(El Bakouri et al. 2009)

Table 3. Comparison of the pseudo-first-order, pseudo-second-order adsorption rate constants and calculated and experimental q_e values attained at different initial carbaryl contents

Initial concentration(mg/L)	$q_{e.exp}$ (mg/g)	Pseudo-first-order kinetic model			pseudo-second-order model		
		k_1	$q_{e.cal}$ (mg/g)	R^2	k_2	$q_{e.cal}$ (mg/g)	R^2
5	24.5	0.084	7.5	0.8162	0.0131	25.52	0.9972
10	35.2	0.035	10.59	0.8173	0.0054	36.78	0.9968
20	90	0.086	49.21	0.8764	0.0017	97.57	0.9922